

Tunable broadband terahertz absorber based on laser-induced graphene

Jingxuan Lan (兰婧萱)¹, Rongxuan Zhang (张荣轩)¹, Hao Bai (白灏)¹, Caidie Zhang (章彩蝶)¹, Xu Zhang (张绪)¹, Wei Hu (胡伟)², Lei Wang (王磊)^{1,2,3*}, and Yanqing Lu (陆延青)²

¹College of Electronic and Optical Engineering, Nanjing University of Posts and Telecommunications, Nanjing 210023, China

²National Laboratory of Solid State Microstructures, College of Engineering and Applied Sciences, Key Laboratory of Intelligent Optical Sensing and Manipulation, Nanjing University, Nanjing 210093, China

³State Key Laboratory of Millimeter Waves, Southeast University, Nanjing 210096, China

*Corresponding author: wangl@njupt.edu.cn

Received March 3, 2022 | Accepted April 24, 2022 | Posted Online May 24, 2022

Terahertz (THz) absorbers for imaging, sensing, and detection are in high demand. However, such devices suffer from high manufacturing costs and limited absorption bandwidths. In this study, we presented a low-cost broadband tunable THz absorber based on one-step laser-induced graphene (LIG). The laser-machining-parameter-dependent morphology and performance of the absorbers were investigated. Coarse tuning of THz absorption was realized by changing the laser power, while it was fine-tuned by changing the scanning speed. The proposed structure can achieve over 90% absorption from 0.5 THz to 2 THz with optimized parameters. The LIG method can help in the development of various THz apparatuses.

Keywords: terahertz; absorber; laser-induced graphene.

DOI: [10.3788/COL202220.073701](https://doi.org/10.3788/COL202220.073701)

1. Introduction

Terahertz (THz) radiation refers to electromagnetic waves ranging from 0.1 to 10 THz. The evolution of THz technology has inspired many innovative THz applications in various areas, including communication, imaging, and astronomy^[1–3]. In all proposed applications, adequate optical components, such as modulators^[4,5], filters^[6–8], and absorbers^[9–12], are in high demand for flexible adaptive control of the electromagnetic properties of THz radiation^[13,14]. The THz metamaterial absorber (TMA), as one of the most important components in THz system applications, has evoked widespread concerns since the first TMAs were proposed by Landy *et al.* in 2008^[15,16]. However, the number of absorbers previously proposed is limited by high manufacturing costs and limited absorption bandwidths^[17–19].

In 2014, a new method called laser-induced graphene (LIG) was proposed^[20]. Compared with traditional synthesis, which requires strict temperature conditions and multiple chemical processes^[21,22], LIG synthesizes patterned carbon composites at room temperature using a simple process through the conversion of commercial polyimide (PI) under direct laser scribing. The discovery of LIG has inspired many applications, including sensors^[23], supercapacitors^[24], and electrodes^[25]. Traditional gratings and Fresnel zone plates for THz modulation have been reported using 450 nm laser writing on a PI film, which indicates

that the LIG method is a promising fabrication method for THz devices^[26]. Recently, we also demonstrated a THz bandstop filter based on the LIG method^[27]. However, to the best of our knowledge, THz absorbers using the LIG method have not been reported.

In this study, we propose a THz graphene grid absorber fabricated through the LIG method using a CO₂ laser. The properties and morphology of the graphene grid can be adjusted by controlling the laser power and scanning speed during fabrication. Thus, tunable THz absorption can be achieved. The absorber can achieve a high absorption of over 90% in the range of 0.5 THz to 2 THz with optimized laser machining parameters.

2. Experimental Details

A schematic of the fabrication process is shown in Fig. 1(a). A CO₂ laser processing system with a focal spot size of 50 μm and wavelength of 10.6 μm was used to induce the graphene grid. The power of the CO₂ laser can be shifted continuously from 0.01 to 30 W, and the scanning speed of the laser is also tunable. A PI film with a thickness of 50 μm was adhered to the Al substrate. The graphene grid was formed by laser scribing the PI film directly. As shown in Fig. 1(b), the absorber removed from the Al substrate consisted of two layers. The top layer of grid-patterned graphene was produced from the PI film. The bottom

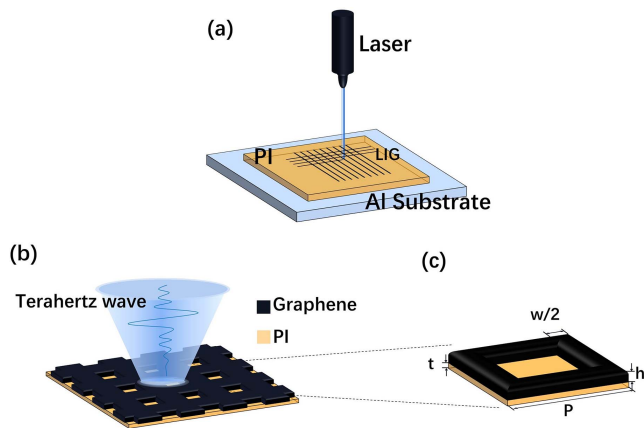


Fig. 1. (a) Schematic of LIG fabrication. (b) Grid graphene THz absorber. (c) Unit cell of the absorber.

layer is the residual PI film, which supports the flexibility of the THz graphene grid absorber. The morphology and properties of graphene can be changed by varying its machining parameters. Thus, the incident THz waves were absorbed at different levels. Figure 1(c) shows the unit cell of the grid. The period, P , of the basic structural unit was designed to be $450\ \mu\text{m}$. The thickness and width of the graphene stripe were changed by changing the laser power and scanning speed. Additionally, to improve the quality of the grid graphene, we used multiple lasing^[28]. All fabricated samples were induced three times.

3. Results and Discussion

Figure 2(a) shows one of the fabricated samples. The microscopic image of the sample is shown in Fig. 2(b). The sample was induced with a laser power of $24\ \text{W}$ and scanning speed of $230\ \text{mm/s}$. Thereafter, we used a Raman spectrometer to

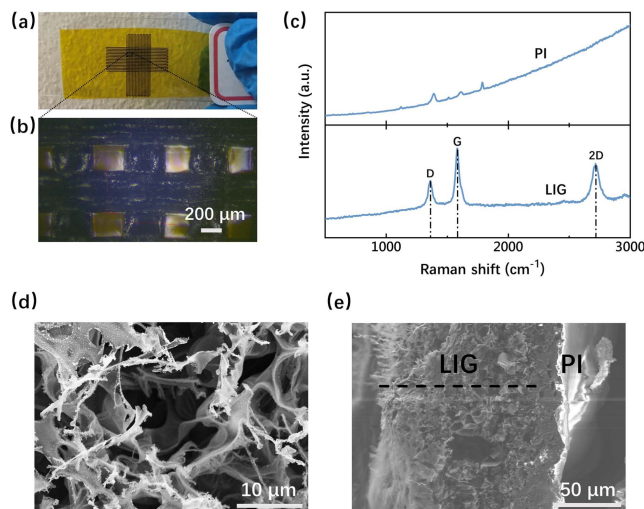


Fig. 2. (a) Sample of the LIG absorber. (b) Graphene grid observed under a microscope. (c) Raman spectra of the LIG and PI. (d) SEM image of the LIG. (e) SEM image of the cross section of the LIG.

measure the Raman spectra of the samples. Figure 2(c) shows the Raman spectra of LIG and PI. The LIG Raman spectra depicted in Fig. 2(c) illustrate the D, G, and 2D peaks at 1359 , 1583 , and $2713\ \text{cm}^{-1}$, respectively, indicating that the PI was converted into graphene under the laser machining parameters. Using a scanning electron microscope, we observed the surface and cross-sectional morphologies of the LIG. The porous microstructure of graphene is shown in Fig. 2(d). The thickness of the generated LIG is shown in Fig. 2(e); the PI film is quite thin compared with LIG, indicating that most of the PI was converted to LIG.

To investigate the relationship between the performance of the absorber and laser power, the temporal spectra of the absorbers with different laser powers were measured using a THz time-domain spectroscopy system (THz-TDS, TAS7400SP; Advantest Corporation) with a transmission analysis accessory. We set the laser power to range from 40% to 80% of the maximal laser power ($P_{\text{max}} = 30\ \text{W}$), with a fixed scanning speed of $230\ \text{mm/s}$. From the inset of Fig. 3(a), it is clear that when the laser power reaches 40% of P_{max} , the spectrum of the THz wave shifts slightly without any change compared with that of the pristine PI film. With an increase in laser power, the intensities of the THz waves gradually weaken. The frequency-dependent transmittances (T) of the absorbers formed at different laser powers are shown in Fig. 3(b). The transmittance is nearly zero at 80% P_{max} . The transmittances of the absorbers increased with a decrease in laser power. The small peaks in the curves at 40% and 50% may be related to the PI material. THz-TDS with a reflectance analysis accessory was employed to characterize the properties of the THz reflectance (R) of the absorbers. All absorbers processed with different laser powers have low reflectivity, as shown in Fig. 3(c). There are only small peaks at $1.3\ \text{THz}$ on the curves of 50% and 60% owing to weak resonances of the grid structures, indicating that the devices have good anti-reflection performance based on the LIG method. Therefore, laser power-dependent absorption (A) spectra ($A = 1 - T - R$)

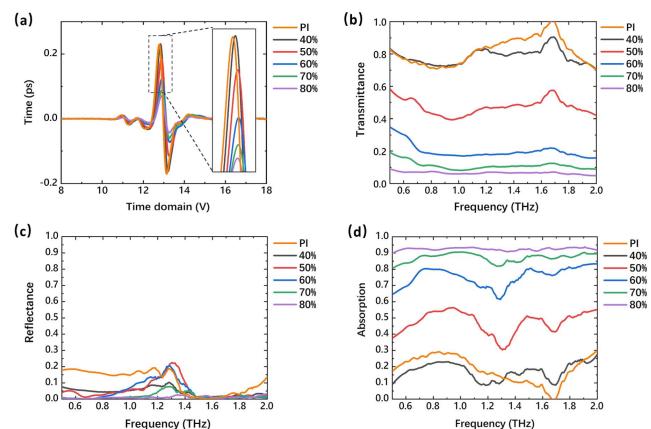


Fig. 3. (a) Time-domain results of the THz graphene grid absorbers induced by the different laser power ranging from 40% to 80%. (b) Corresponding transmittance spectra, (c) reflectance spectra, and (d) absorption spectra of the absorbers.

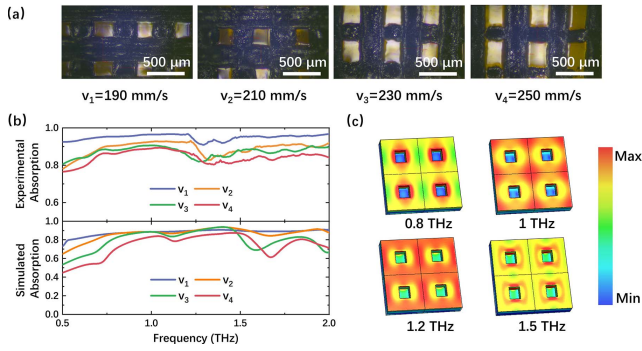


Fig. 4. (a) Graphene grid absorbers induced with different laser scanning speeds under a microscope. (b) Corresponding experimental and simulated absorption spectra of the absorbers. (c) Simulated THz near-field distributions of the absorber ($W = 300 \mu\text{m}$) at a frequency of 0.8 THz, 1 THz, 1.2 THz, and 1.5 THz, respectively.

were obtained, as shown in Fig. 3(d). It was found that the absorption can be adjusted widely from 10% to 90% with a laser processing power from 40% to 80%. A well-performed broadband THz graphene grid absorber with absorption over 90% from 0.5 THz to 2.0 THz is achieved with the 80% of P_{max} and scanning speed of 230 mm/s. High-quality LIG with high conductivity produced by an enhanced laser power and the porous structure of graphene makes the device have high THz absorption.

Next, the laser-scanning-speed-dependent morphology and THz absorption of the graphene grid absorbers were characterized. We changed the laser scanning speed from 190 mm/s to 270 mm/s when the laser power was fixed at 70% of P_{max} . The influence of the laser scanning speed on the unit structure of the absorber was demonstrated using an optical microscope, as shown in Fig. 4(a). When the scanning speed increases, the grid width decreases, making the center part of the PI unit larger, and thus less PI is converted into graphene. Therefore, more THz waves are allowed to pass through. Moreover, we used the THz-TDS system to measure the transmittance and reflectance of graphene grids (not shown). The absorption spectra obtained are shown in Fig. 4(b). Unlike the curves in Fig. 3(d), there is only a slight change in absorption range from 0.8 to 0.9 with different laser scanning speeds. The small asymmetry in the grid owing to the LIG method had a slight effect on the absorption characteristics. Furthermore, all the LIG grid absorbers mentioned in this paper exhibited excellent polarization-independent absorption in the THz range. A commercial electromagnetic solver (CST Microwave Studio 2018) was used for simulations. The PI spacer is considered a lossy material with a dielectric constant of $\epsilon = 3.23$ and dielectric loss tangent of $\tan \delta = 0.033$. The dielectric constant of the induced graphene was set to 2.4 with a dielectric loss tangent of 0.99. All of these values were obtained from the THz-TDS system. The thickness of the graphene grid was set as $145 \mu\text{m}$. We changed only the size of the structural unit corresponding to different laser scanning speeds. The simulated absorptions agreed well with the

experimental results. Consequently, the feasibility of fine tuning the THz absorption characteristics using the laser scanning speed to adjust the size of the structural unit is proven. Figure 4(c) illustrates the simulated THz near-field distributions of the proposed absorber. The THz radiation was absorbed by the graphene grid. Different regions of graphene absorb THz waves at different frequencies.

We obtained two broadband LIG grid absorbers with a good performance of 90% absorption from 0.5 THz to 2 THz. One was induced with a laser power of 70% and scanning speed of 190 mm/s, and the other was induced with a laser power of 80% and scanning speed of 230 mm/s. This can be proven from the laser flux Φ formula^[26]:

$$\Phi = \frac{P}{v \times d}, \quad (1)$$

where P is the laser power, v is the scanning speed, and d is the diameter of the laser spot.

The laser flux is a key factor in THz absorption. When d is fixed, both low-power, low-speed, and high-power, high-speed lasers can achieve the same THz absorption. However, the laser power has a greater influence on THz absorption. More heat generated by the high-power laser is exposed to the PI film, breaking the C – O, C = O, and N – C bonds in PI and inducing additional graphene. Higher-quality LIG can be produced by a higher laser power. The scanning speed affected the accumulation and diffusion of the generated heat. A low scanning speed causes more heat accumulation and diffusion, and thus the grid widths of the LIG absorber increase. Therefore, we can realize coarse tuning of the THz absorption by changing the laser power while fine tuning by changing the scanning speed. In addition, we fabricated graphene films without a grid structure using the LIG method for comparison with our graphene grid absorbers. Although the graphene film can also achieve broadband absorption, the THz reflectance of the graphene film was larger. The grid structure has higher THz absorption, is more flexible, and is not easy to break. In addition, we can optimize the THz absorption characteristics by controlling the unit size of the grid structure of the absorber using laser machining parameters.

4. Conclusion

A grid graphene broadband absorber for the THz range was proposed based on the LIG method. We investigated the influence of varying laser power and scanning speed on the absorber performance. It was found that we can coarsely tune the absorption by changing the laser power and subtly tune the absorption by changing the scanning speed. With optimized parameters, the fabricated absorber exhibited a high absorbing capacity of over 90% within a broad bandwidth ranging from 0.5 to 2 THz. Furthermore, the grid structure of our absorber makes the device more robust and flexible than an unpatterned LIG film. Through this easy and cost-effective LIG method, various

carbon-based THz devices are expected, such as filters and modulators, which may have great potential in numerous applications, ranging from THz communication to THz imaging and sensing.

Acknowledgement

This work was supported by the Natural Science Foundation of Jiangsu Province (No. BK20211277), the China Postdoctoral Science Foundation (Nos. 2019M651768 and 2020T130285), the Natural Science Foundation of Jiangsu Province Major Project (No. BK20212004), the Fundamental Research Funds for the Central Universities (No. 021314380095), and the Open Foundation of State Key Laboratory of Millimeter Waves (No. K202226).

References

1. J. Federici and L. Moeller, "Review of terahertz and subterahertz wireless communications," *J. Appl. Phys.* **107**, 111101 (2010).
2. M. Tonouchi, "Cutting-edge terahertz technology," *Nat. Photonics* **1**, 97 (2007).
3. T. Nagatsuma, G. Ducournau, and C. C. Renaud, "Advances in terahertz communications accelerated by photonics," *Nat. Photonics* **10**, 371 (2016).
4. Y. Shen, Z. Shen, G. Zhao, and W. Hu, "Photopatterned liquid crystal mediated terahertz Bessel vortex beam generator," *Chin. Opt. Lett.* **18**, 080003 (2020).
5. H. T. Chen, W. J. Padilla, M. J. Cich, A. K. Azad, R. D. Averitt, and A. J. Taylor, "A metamaterial solid-state terahertz phase modulator," *Nat. Photonics* **3**, 148 (2009).
6. H. Zhuang, C. Liu, F. Li, J. Zhuang, and K. Li, "Tunable plasmonic filter based on parallel bulk Dirac semimetals at terahertz frequencies," *Appl. Opt.* **60**, 3634 (2021).
7. H. Sun, J. Yang, H. Liu, D. Wu, and X. Zheng, "Process-controllable modulation of plasmon-induced transparency in terahertz metamaterials," *Chin. Opt. Lett.* **19**, 013602 (2021).
8. Y. Chen, J. Li, C. He, J. Qin, X. Chen, and S. Li, "Enhancement of high transmittance and broad bandwidth terahertz metamaterial filter," *Opt. Mater.* **115**, 111029 (2021).
9. H. Deljoo and A. Rostami, "Broadband terahertz absorber using superimposed graphene quantum dots," *Opt. Quantum Electron.* **53**, 442 (2021).
10. J. Bai, Z. Pang, P. Shen, T. Chen, W. Shen, S. Wang, and S. Chang, "A terahertz photo-thermoelectric detector based on metamaterial absorber," *Opt. Commun.* **497**, 127184 (2021).
11. Z. Shen, S. Li, Y. Xu, W. Yin, and X. Chen, "Three-dimensional printed ultra-broadband terahertz metamaterial absorbers," *Phys. Rev. Appl.* **16**, 014066 (2021).
12. J. Xiao, R. Xiao, R. Zhang, Z. Shen, W. Hu, L. Wang, and Y. Lu, "Tunable terahertz absorber based on transparent and flexible metamaterial," *Chin. Opt. Lett.* **18**, 092403 (2020).
13. M. Rahm, J. S. Li, and W. J. Padilla, "THz wave modulators: a brief review on different modulation techniques," *J. Infrared Millim. Terahertz Waves* **34**, 1 (2012).
14. K. D. Xu, J. Li, A. Zhang, and Q. Chen, "Tunable multi-band terahertz absorber using a single-layer square graphene ring structure with T-shaped graphene strips," *Opt. Express* **28**, 11482 (2020).
15. T. Hu, N. I. Landy, C. M. Bingham, X. Zhang, R. D. Averitt, and W. J. Padilla, "A metamaterial absorber for the terahertz regime: design, fabrication and characterization," *Opt. Express* **16**, 7181 (2008).
16. F. J. Bosquespadilla, L. N. Landy, W. K. Smith, J. D. Smith, E. Padilla, and S. Sajuyigbe, "Perfect metamaterial absorber," *Phys. Rev. Lett.* **100**, 207402 (2008).
17. J. Huang, T. Fu, H. Li, Z. Shou, and X. Gao, "A reconfigurable terahertz polarization converter based on metal-graphene hybrid metasurface," *Chin. Opt. Lett.* **18**, 013102 (2020).
18. X. Shen, Y. Yang, Y. Zang, J. Gu, J. Han, and W. Zhang, "Triple-band terahertz metamaterial absorber: design, experiment, and physical interpretation," *Appl. Phys. Lett.* **101**, 207402 (2012).
19. J. Grant, Y. Ma, S. Saha, A. Khalid, and D. R. Cumming, "Polarization insensitive, broadband terahertz metamaterial absorber," *Opt. Lett.* **36**, 3476 (2011).
20. J. Lin, Z. Peng, Y. Liu, F. Ruiz-Zepeda, R. Ye, E. L. G. Samuel, M. J. Yacaman, B. I. Yakobson, and J. M. Tour, "Laser-induced porous graphene films from commercial polymers," *Nat. Commun.* **5**, 5714 (2014).
21. A. K. Geim and K. S. Novoselov, "The rise of graphene," *Nat. Mater.* **6**, 183 (2007).
22. W. Liu, J. Wei, X. Sun, and H. Yu, "A study on graphene-metal contact," *Crystals* **3**, 257 (2013).
23. M. G. Stanford, K. Yang, Y. Chyan, C. Kittrell, and J. M. Tour, "Laser induced graphene for flexible and embeddable gas sensors," *ACS Nano* **13**, 3474 (2019).
24. Z. Peng, J. Lin, R. Ye, E. Samuel, and J. M. Tour, "Flexible and stackable laser-induced graphene supercapacitors," *ACS Appl. Mater. Interfaces* **7**, 3414 (2015).
25. M. G. Stanford, J. T. Li, Y. Chyan, Z. Wang, and J. M. Tour, "Laser-induced graphene triboelectric nanogenerators," *ACS Nano* **13**, 7166 (2019).
26. Z. Wang, G. Wang, G. Liu, B. Hu, and Y. Zhang, "Patterned laser-induced graphene for terahertz wave modulation," *J. Opt. Soc. Am. B* **37**, 546 (2020).
27. R. Zhang, G. Zong, S. Wu, R. Song, X. Zhang, S. Ge, W. Hu, L. Wang, and Y. Lu, "Ultrathin flexible terahertz metamaterial bandstop filter based on laser-induced graphene," *J. Opt. Soc. Am. B* **39**, 1229 (2022).
28. Y. Chyan, R. Ye, Y. Li, S. P. Singh, C. J. Arnsch, and J. M. Tour, "Laser-induced graphene by multiple laser: toward electronics on cloth, paper, and food," *ACS Nano* **12**, 2176 (2018).